International Journal of Thin Films Science and Technology

http://dx.doi.org/10.18576/ijtfst/090306

Optimization of LDM 3D printing parameters for TiO_2 thin film fabrication

Aran Hansuebsai [1,*], *Krairop Chareonsopa* [1] *and Kazuhiro Manseki* [2]

[1]Department of Imaging and Printing Technology, Faculty of Science, Chulalongkorn University, Bangkok, Thailand.
[2]Faculty of Engineering, Gifu University, Japan.

Received: 2 May 2020, Revised: 2 Jun. 2020, Accepted: 7 Aug. 2020.
Published online: 1 Sep. 2020.

Abstract: With the development of 3D printing technology, the application of liquid deposition modeling (LDM) 3D printing has become more and more widespread. Our study aims to use this printer type to fabricate TiO_2 paste on an electrode for Dye Sensitized Solar Cell (DSSC). As the paste showed a shear-thinning behavior, the printing test was carried out to investigate the effects of printer's parameters setting on the thin film characteristics. A number of successive layers was also considered to ensure the quality of printing. The critical thickness of TiO_2 thin films and relevant sheet resistance in this system were achieved at 6.25 μm and 6.8E+6 Ω/square, respectively. Examples of DSSC directly formed upon the obtained thin films were presented, by which the energy conversion efficiency was received at approximately 4%. This approach opens the way to the direct deposition of nano-TiO_2 paste by means of a low-cost LDM 3D printer. It includes the product development in different patterns and shapes of printed thin films.

Keywords: 3D printing, Liquid deposition modeling, DSSC, TiO_2 thin film

1 Introduction

Since the pioneering work of O'Regan and Grätzel in 1991 [1], there has been a great interest in Dye Sensitized Solar Cell (DSSC) by the research community. This technology is based on cells made of two opposite conductive substrates: the first one (photo electrode) is coated with porous nano-crystalline TiO_2, while the second one (counter electrode) is coated with Pt or graphite. The electrodes can be glasses. These glasses are covered with a transparent conductive oxide (TCO) of a thickness lower than 1 μm, usually a fluorine doped tin oxide (FTO) is used.

Dye molecules are adsorbed on TiO_2 by dipping the photo-anode into a dye solution. The electrons of these molecules, excited by light, are infused into the conduction band of TiO_2 and subsequently transferred to the FTO that attaches on the glass. The electrons can be recovered by a redox reaction with the electrolytic solution enclosed into the cell. The reduction of the electrolyte occurs at the counter electrode catalyzed by the Pt.

DSSC can be designed in several types. The most popular one is composed of three parts: a dye-sensitized nano-crystalline thin film photo-anode, a redox couple (usually I_3^-/I^-) in organic solvent(s), and a platinized transparent conducting oxide glass as a counter electrode. It should be noted that the iodine–iodide redox electrolytes may have some disadvantages such as its oxidizing nature, especially in the presence of moisture, photocurrent loss due to visible light absorption and significant loss in short circuit current density, particularly in highly viscous electrolytes [2]. Accordingly, another type of DSSC is proposed as solid-state dye-sensitized solar cells.

Interestingly, the characteristics of thin film on electrodes will pave a new way to develop, more efficiently of, all types of DSSC, opening up a new perspective for industry. Several materials can be used as a thin film such as TiO_2, SiO_2 and so on. Among those materials, TiO_2 is an attractive material to apply for most DSSCs, as it does not only have a high refractive index, but also for being a hydrophilic property [3].

To consider the fabricating techniques, a broad range of methods has been developed with different capabilities, as their fundamentals are diverse. Screen printing, inkjet printing, and solid freeform fabrication (SFF) technologies such as stereo-lithography, selective laser sintering, selective

*Corresponding author E-mail: aran.h@chula.ac.th

laser melting and fused deposition modeling (FDM) are among the most widely used in thin film fabrication, as they possibly control film thickness and its porosity [4-9]. SFF methods are based on the principle of three-dimensional (3D) printing.

The existence of these technologies differ in terms of cost, maximum spatial resolution and type of materials used. For example, the FDM technology was recently demonstrated to fabricate the electronic sensors [10]. However, it still requires the additional step of the production of a solid composite filament to be heated and melted in order to be processed with a standard FDM 3D printer.

Liquid deposition modelling (LDM) has emerged as an alternative and a cost-effective technique to overcome some of the limits imposed by the FDM approach [11]. The concept is the additive deposition of material layers directly from a fluid-dense materials in a volatile solvent. By means of this technology, the production of freeform structures was achieved by using an extruding nozzle and a computer-controlled robot moving along the x, y and z axes.

Using LDM technique, the rheological behavior of dispersed micro or nano-particles is important, and their printability must be identified based on the shear-rate of the material at the extrusion nozzle. It is noted that we may call this methodology, in another term, as "low temperature deposition manufacturing", as there is no need to use a solid filament like FDM technique. Using a uniform homogeneous dispersion of liquid/paste is a key factor of 3D printing. It is because of the high tendency of particles to form bundles and aggregates that may cause clogging of the nozzle and flux instability during the printing process. In addition, printing speed and shear-rate of the dispersion at the extrusion nozzle needs to be controlled. Therefore, an appropriate material concentration is required to obtain a thin film without the fracture of surface. The first attempt to print conductive thin film by means of LDM technique was described by Giovanni et al. [12]. They used polymeric nanocomposite liquid dispersions based on poly(lactic acid) (PLA) and multi-walled carbon nanotubes (MWCNTs).

Our research studied the effect of the LDM 3D printer's parameters on the quality of nano-TiO_2 thin films. The printers' parameters such as nozzle size, printing speed, air pressure and the distance between the nozzle tip and an electrode's surface were investigated, to optimize the setting of the printer. The thin film characteristics such as thickness, uniformity, surface roughness, crack-free, resistivity and photovoltaic efficiency were observed. This research will be of useful for scientists who are engaged with DSSC.

1.1 3D Printing

"3D printing" is a common name under the SFF technique. Some industries refer to 3D printing system as Additive Layer Manufacturing (ALM), but we will use its practical name here—3D Printing. There are different types of 3D printers, depending on cost, print quality, maximum speed, capability, practicality and user expectations.

The technologies and materials used are varied, including the way of materials extrusion to substrates. The machines are no longer difficult for home users, such as the users can create a virtual design (3D model) of the object they want to print in three dimension; and they can save their design as a Computer Aided Design file, or CAD. The advantages of this printing system include the ability to vary the number of printed layers as well as different levelling pattern of thin films by one time operation.

Liquid Deposition Modeling (LDM) printer was in our interest, as its extruder could be used for thin film fabrication, by using paste materials like clay, alumina and TiO_2. It can be based on a pneumatic system in which a pump pushes the paste through the extruder. With this technology, it is possible to accurately control the flow of material and also use retraction to interrupt deposition.

2. Experimental Section

2.1 LDM 3D printer assembly

The printer has three major parts: main board, software and fixed frame. Main board or electrical part is the heart of the system. It controls stepper motors for moving the nozzle in X and Y directions, moving the bed in Z direction and extruding the material from the nozzle. The software which connects to the board through USB interface is used for loading the 3D model file for printing and testing various operations. Fixed frame consists of all necessary components in the system.

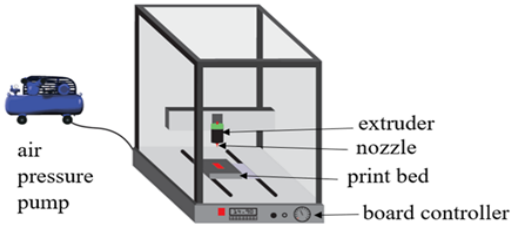

Figure 1. Model of LDM 3D printer

The design was based on a pneumatic system in which the air pressure extruded the TiO_2 paste through the nozzle. Figure 1 shows the assembled LDM 3D printer in the 400 x 350 x 600 mm3 fixed frame with following components:

- *print bed*
- *syringe extruder* – a part, incorporated with a pump, that ejects TiO_2 to deposit it in successive layers on bed.

- *nozzle* – a part that actually extrudes the paste to build the thin film .

- *board controller* – a part responsible for the electronic functioning of the printer.

The overall system was powered by 220 Volts power supply. In addition, 3D software (123D Design) was used to calibrate the machine and to define the printed area and the distance between the print bed and nozzle.

2.2 Preparation of TiO_2 paste

TiO_2 paste (PST-18NR) was purchased from JGC Catalysts and Chemicals Co., Ltd (Japan) with a concentration of 15.8 wt% of TiO_2 and 20 nm particle size. It was based on Anatase phase. The company specializes in surface modification technology to control disperse ability to avoid flocculation during the use of nano-particles, and mixing technology to prepare the paste.

As the original paste was so viscous that it was difficult to flow through the nozzle of LDM 3D printer. To become fluid-dense material, the paste, accordingly, was diluted by adding ethanol 99.5%. However, the diluted paste should be able to support the weight of its own layers, as objects that are too fluid can collapse under their own weight. Viscosity of the paste or resistance to deformation by shear rate shall be considered.

Paste preparation was designated as *x-TiO_2*, where *x* is the weight ratio of ethanol:TiO_2. Three different mixtures were prepared as following: *0.1-TiO_2, 0.16-TiO_2* and *0.25-TiO_2*, respectively. After mixing in a container, agitation was done by a shaker for each sample at room temperature for one hour. Rheological property of each sample was measured by a Malvern Bohlin Gemini HR Nano Rheometer. The measurement was done under controlled speed range from 0.01 milli rad/s to 500 rad/s, yielding plots of the shear stress and viscosity as a function of shear rate at 25°C. The viscosity of these samples was reported at a shear rate of 1.0 s^{-1}.

2.3 Printing test

A printing test was carried out by varying the printer's parameters such as nozzle size, printing speed and air pressure; and to observe the quality of printed films on a TCO glass. According to the printer setting, firstly, the machine was started by leveling the bed to ensure the distance from the tip of the nozzle. Then, the adjustment of each parameter was varied as the following:

- *nozzle size*: 0.42, 0.53, 0.63 and 0.70 mm diameters. (Figure 2)

- *air pressure*: 1, 2, 3, 4, 5 and 6 bars.

- *printing speed*: 5, 15, 25, 35, 40, 60, 80 and 100 mm/s.

Figure 2. Nozzle sizes

After printing, the printed samples were kept in a closed chamber for a while in order to let the wet thin film relax and to reduce the surface irregularity, and then heat treated on a hot plate at 150 °C for 5 min. Later, the samples were gradually heated in an oven up to 500 °C for 4 hrs. A solid self-standing thin film was obtained. An optical microscopy was employed to evaluate the uniformity and crack of the printed films. The proper combinations of these parameters and *x-TiO_2* paste were considered to achieve the uniform printed TiO_2 films without crack.

2.4 Thin film fabrication

Printer setting from 2.3 was chosen for fabricating the thin films. The *x-TiO_2* paste was printed directly on the TCO glass (Nippon glass 4 mm thickness with sheet resistance 11 Ω/square) with an effective area of 5 x 5 mm^2, representing as the photo-electrode of DSSC. The number of laid down layer was designed as 1-4 layers, as shown in Figure 3. Other designs included different shapes and layers with disconnected and connected patterns, as shown in Figure 4. The data files were created and sent to the printer. After baking, the surface characteristics of TiO_2 thin films such as uniformity, crack, thickness and roughness were observed by eyes and measured by SEM and a 3D laser microscope. We also measured sheet resistance of these thin films by using a SourceMeter model 2450 with a Four-Point Collinear Probe.

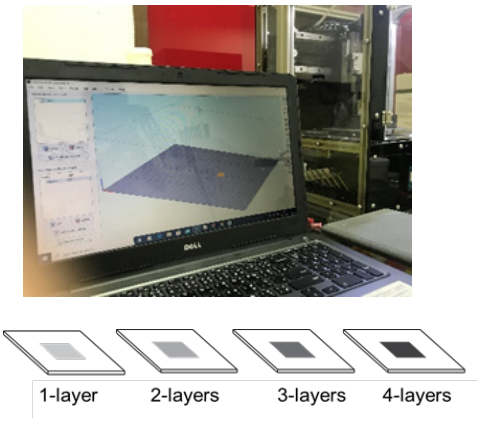

Figure 3. Printed area and laid down layers designed by an Autodesk 123D Design software

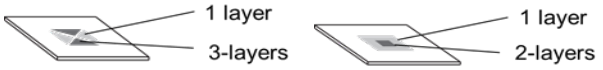

Disconnected pattern Connected pattern

Figure 4. Different shapes and pattern designs of thin films

2.5 DSSC assembly

The printed TiO_2 electrode samples were immersed into a dye solution consisting of D205 dye (Chemicrea Co.,Ltd) of 0.0087 grams and Chenodeoxycholic acid of 0.0080 grams in a mixture of acetonitrile super dehydrate of 25 ml. and tert-butyl alcohol (2-methyl-2-propanol) of 25 ml, for 4 hours. To prepare the counter electrode (TCO glass), a hole was drilled in the electrode. After removing the residual contaminant, Pt catalyst was deposited on the glass by an Ion Coater (Eiko IB-3).

A dye-covered printed TiO_2 electrode sample and Pt-counter electrode were assembled into a sandwich type cell and sealed with a two-side glue coated tape of 1 mm thickness. A drop of the electrolyte containing fluid I^-/I_3^- redox couples was put into the hole of the cell by vacuum backfilling techniques. The holes were then sealed by using polymer foils (Surlyn). Figure 5 represents the schematic diagram of DSSC assembly. Finally, the overall light-to-electric energy conversion yield of DSSC was measured by a solar simulator.

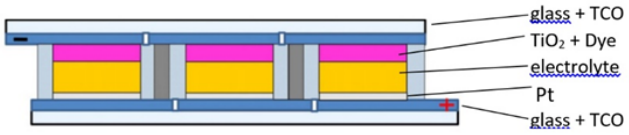

Figure 5. Schematic diagram of DSSC assembly

3. Results and discussion

3.1 Rheology of x-TiO_2 paste

We found the decline in viscosity of *x-TiO_2* paste by dilution effect as follows: 130, 72, 59 and 46 Pas for original TiO_2, *0.1-TiO_2*, *0.16-TiO_2* and *0.25-TiO_2*, respectively. Interestingly, viscosity-shear rate dependence of these *x-TiO_2* pastes, as shown in Figure 6, represents all curves in a similar manner; that is, the decrease in viscosity as shear rate increases indicated shear thinning behavior. This is typical of paste with high solid content system. The higher the solid content is, the stronger the change of viscosity becomes. Similar manners were also found by using other geometries of measurement. The paste, accordingly, represented non-linearity of viscosity on share rate dependence. In addition, it was found that the viscosity of paste increased at higher temperatures, as its behavior upon evaporation gave continuous change from liquid state to pseudo-liquid state, close to solid on flow. The measurement suggested that the paste had visco-elastic property. This behavior would relate to the adjustment of printer's parameters, such as printing speed and air pressure.

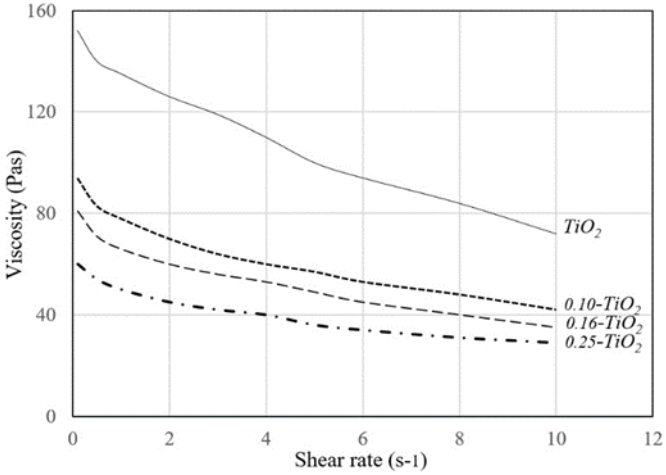

Figure 6. Viscosity vs shear rate curves of *x-TiO_2* pastes

3.2 Printer setting vs print quality

TiO_2 thin film electrodes could fracture during baking above a critical film thickness. Clearly, cracking in the film was affected by substantial sliding at the interface, which created wide open crack surfaces, exposing the underlying substrate [13]. Accordingly, to consider the setting of 3D printer, it should be based on the critical thickness of thin film, which represents no crack after baking.

Regarding the distance between the tip of the nozzle and the electrode surface, shorter distance seems to give a satisfied surface finish. Longer distance results in an irregular surface by which a crack could be occurred. Based on the printing test, we proposed a variable distance relevant to the nozzle size. These values were not the standard, but could be the rule of thump that the distance should be half of the used nozzle size.

To select the nozzle size, in general, the larger nozzle size gives thicker film thickness by which the crack of TiO_2 film can be easily occurred. The smaller size may be suitable to achieve thinner films without a crack. However, the right selection shall relate to the combination of 3D printer's parameters such as air pressure and printing speed by which the proper amount of extruded TiO2 paste will be obtained to not form over the critical film thickness. Figure 7 shows some enlarged images of 1-layer printed thin films through the optical microscope using *0.1-TiO_2* paste, by a different parameters setting. It should be noted that cracked and crack-free printed thin films were included. Similar tests were done with *0.16-TiO_2* and *0.25-TiO_2* paste samples, respectively.

From the experimental data analysis, we can see that when the nozzle size becomes larger, the printing speed should be increased together with the decreased air pressure in order to control the proper amount of extruded paste. In addition, the incline of paste viscosity showed the similar trend. Data of parameters setting based on the change of nozzle size and *x-TiO_2* paste are given in Table 1.

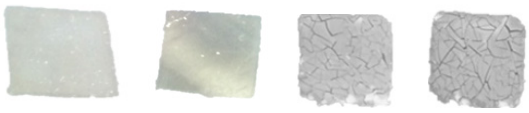

0.42 mm 0.53 mm 0.63 mm 0.7 mm
(different nozzle size)

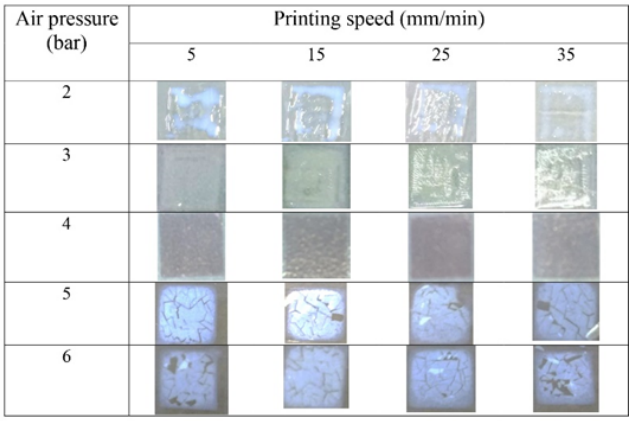

Figure 7. Enlarged images of printed films using *0.1-TiO_2* paste with nozzle size 0.42 mm (x50)

Table 1. Printer's parameters setting on nozzle size dependence

	Printing speed (mm/sec)		
Nozzle size (mm)	*0.10-TiO_2*	*0.16-TiO_2*	*0.25-TiO_2*
0.42	5-40	35-40	60
0.53	↓	↓	↓
0.63	↓	↓	↓
0.70	60-100	80-100	100

	Air pressure (bar)		
Nozzle size (mm)	*0.10-TiO_2*	*0.16-TiO_2*	*0.25-TiO_2*
0.42	3-4	2-3	2
0.53	↑	↑	↑
0.63	↑	↑	↑
0.70	1-2	1	1

Printer setting plays an important role in controlling the surface finish of wet thin films. Too low air pressure gives non-uniform surfaces. While too high air pressure compresses the deformation of these layers. A flick of the TiO_2 paste from the nozzle tip tends to occur when the printing speed increases. This uneven surface's feature activates easily the crack of layers after baking. Accordingly, we recommend that the moderate values of these printer's parameters are important. It was suggested that the *0.1-TiO_2* paste and 0.42 mm nozzle size be suitable for fabricating the *TiO_2* thin films, as the printer's parameters setting fell in the moderate values with larger tolerance. Result shows that the air pressure setting at 4 bar gives the crack-free and uniform TiO_2 layer in the range of printing speeds from 25 to 35 mm/min.

3.3 Thin film characteristics

We found that morphology of the crack-free TiO_2 thin films, significantly unaltered after printing and baking, as shown in Figure 8. SEM micrographs were taken at different magnifications to be able to observe its quality. According to the observation, the thin films contained no aggregates and were dispersed homogeneously over the large area, indicating the uniformity of the thin films and the optimization of printer setting.

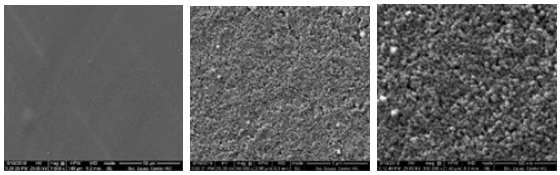

x1,000 x5,000 x10,000

Figure 8. SEM images of morphology of crack-free TiO_2 thin films

From this finding, it can be said that the paste has an appropriate flow property, consistent with the nozzle size, air pressure, printing speed and the distance between the base and the nozzle tip. Result also indicates that there is no change in TiO_2 phase transformation, which has a direct influence on the thickness and surface roughness of the obtained thin films. Cross-sectional image shows the average thickness of these 1-layer thin films is approximately 5 μm and their RMS surface roughness is 0.70 μm measured by SEM and 3D laser microscope, respectively, as shown in Figure 9.

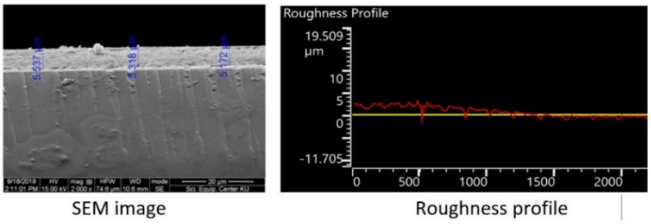

Figure 9. SEM image and roughness profile of 1-layer TiO2 thin film (nozzle size 0.42 mm, air pressure 4 bar, printing speed 25 mm/s, distance 0.2 mm)

The porosity of thin film can be observed from SEM images. This was confirmed by baking process, which allowed necking among the TiO_2 particles and burning of solvents and binders. This improved the specific area and electrical conductivity. The measured sheet resistance is approximately 6.57E+6 Ω/square, as shown in Figure 10. Note that most of the printed *0.1-TiO_2* samples in the range of printing speed 5-35 mm/min give the close values. The porous property of thin films also assists dye molecules to penetrate through these pores, and more molecules could be adsorbed directly onto the surface of thin films. The electrolyte could contact directly the dye molecules through these pores, so that the dye molecules could obtain electrons from the electrolyte, in order to fulfill the photovoltaic conversion process. Our measurement confirmed the achievement of conversion efficiency of DSSC at 4.07% in simulated light.

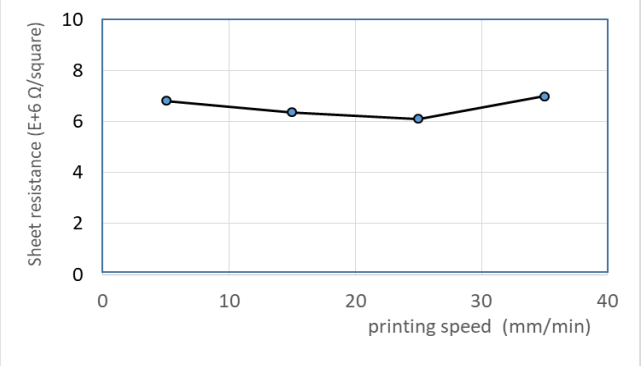

Figure 10. Sheet resistance of printed TiO_2 thin films vs printing speed

3.4 Multi-layers printing and critical film thickness

As mentioned earlier, the interfacial sliding in the *x-TiO_2* paste and printer's parameters strongly influenced the multi-layers printing and critical film thickness for the crack. By this system, we achieved three successive layers without a crack by using *0.1-TiO_2 paste*. The data of film thickness, sheet resistance and conversion efficiency for one to four successive layers are given in Table 2. It was found that the multi-layers printing did not significantly affect the increase of thin film thickness. It was due to the spreading of the extruded paste. However, at the optimum three successive layers, the film thickness was approximately at 6.25 µm. We, accordingly, proposed the value of 6.25 µm as the critical film thickness for the crack. When the thin film thickness is higher than the critical value, the crack can be easily occurred. It should be noted that the measured sheet resistance and conversion efficiency of thin films under the critical film thickness value were acceptable in the standard range. Improving these properties depends on the choice of materials usage.

To consider the advantages of 3D printing, DSSC manufacturers now can use this methodology in product development. For example, a change in printed electrode design is a new challenge to create a customized DSSC product. In our study, we found that the printed TiO_2 thin films in different shapes, patterns and variable successive layers were possible for DSSC applications. Based on our measurement, the overall light-to-electric energy conversion yield was 3.01-3.23% in simulated solar light.

Table 2. Multi-layer printing vs film thickness, sheet resistance and conversion efficiency

number of layer	film thickness (µm)	sheet resistance (Ω/square)	conversion efficiency (%)
1-layer	5.00	6.10E+6	4.07
2-layers	5.88	6.45E+6	4.08
3-layers	6.25	6.8E+6	4.14
4-layers	6.38	167.07E+6	- (crack)

4 Conclusions

In summary, we demonstrated a simple and cheap LDM 3D printer to fabricate the TiO_2 thin film, by using the commercial TiO_2 paste available in the market. Extrusion force is important to control the characteristic of thin film and its quality. This depends on the rheological property of the paste. Based on our experiment, the *0.1-TiO_2* paste and 0.42 mm nozzle size are suitable for fabricating the TiO_2 thin films, as the parameters setting fell in the moderate values with larger tolerance. The critical thin film thickness was confirmed by the value of its sheet resistance (6.8E+6 Ω/square) and the conversion efficiency of DSSC (4%), which fell in the acceptable ranges. The limitation of this system was that the obtained thin film thickness was not as high as we expected (5-6 µm) and the multi-layer printing did not significantly affect the increase of thin film thickness. It was due to the occurrence of spreading phenomenon of the extruded paste. Accordingly, the rheology of the TiO_2 paste should be improved and the range of printer's parameters needs to be enlarged. However, the advantage of this technique will open the new design of printed electrode and its quality guarantee for the performance of DSSC.

Acknowledgement

The authors would like to thank the Department of Imaging and Printing Technology, Faculty of Science, Chulalongkorn University for supporting this research and Gifu University for providing facilities at Prof. Manseki's Laboratory.

References

[1] B. O'Regan, M. Grätzel, A low-cost, high-efficiency solar cell based on dye-sensitized colloidal TiO2 films. *Nature*, **353**, 737–740, (1991)

[2] K. Manseki, W. Jarernboon, Y. Youhai, K.J. Jiang, K. Suzuki, N. Masaki, Y. Kim, J. Xia and S. Yanagida, Solid-state dye-sensitized solar cells fabricated by coupling photoelectro-chemically deposited poly(3,4-ethylenedioxythiophene) (PEDOT) with silver-paint on cathode. *Chemical Communications*, **47 (11),** 3120-3125, (2011)

[3] M.F. Hossain, S. Biswas, T. Takahashi, Y. Kubota and A. Fujishim, Influence of direct current power on the photocatalytic activity of facing target sputtered TiO2 thin films. *Thin Solid Films*, **517(3)**, 1091–1095, (2008)

[4] B.J. De Gans and U.S. Schubert, Inkjet printing of polymer micro-arrays and libraries: Instrumentation, requirements, and perspectives macromolecular. *Rapid Communications*, **24,** 659–666, (2003)

[5] D. Zhang, S. Ito S, Y. Wada, T. Kitamura and S. Yanagida, Nanocrystalline TiO2 electrodes prepared by water-medium screen printing technique. *Chemistry Letters,* **30**, 1042–1043, (2001)

[6] T.K. Gupta, L.J. Cirignano, K.S. Shah, L.P. Moy, D.J. Kelly, M.R. Squillante, G. Entine and G.P. Smestad, Screen-printed dye-sensitized large area nanocrystalline solar cell. *Proc. Material Research Society Symposium*, **581,** 653–658, (2000)

[7] W.Y. Padrón-Hernándeza, M.C. Ceballos-Chuca, D. Pourjafaria, G. Oskama, J.C. Tinocob, A.G. Martínez-Lópezb and G.Rodríguez-Gattornoa. *Stable inks for inkjet printing of TiO_2 thin films*, in Proc. Materials Science in Semiconductor, **81**, 75-81, (2018)

[8] I. Gibson, D.W. Rosen and B. Stucker. *Additive manufacturing technologies – Rapid prototyping to direct digital manufacturing*. New York,„*Springer* (2010)

[9] M. Vaezi and S. Yang. Chapter 2: *Freeform fabrication of nanobiomaterials using 3D printing*, in Book: Rapid prototyping of biomaterials, Woodhead Publishing Limited, Cambridge, 17-74, (2014)

[10] S.J. Leigh, R.J. Bradley, C.P. Purssell, D.R. Billson and D.A. Hutchins, A Simple, low-cost conductive composite material for 3D printing of electronic sensors. *PLoS ONE*, **7(11)**, e49365, (2012)

[11] S.Z. Guo, F. Gosselin, N. Guerin, A.M. Lanouette, M.C. Heuzey and D. Therriault, Solvent-cast three-dimensional printing of multifunctional microsystems, Small (Macro and Nano). *Wiley Online Library*, **9(24)**, 4118–22, (2013)

[12] G. Postiglione, G. Natale, G. Griffini, M. Levi and S. Turri, Conductive 3D microstructures by direct 3D printing of polymer/carbon nanotube nanocomposites via liquid deposition modeling. *Composites: Part A*, **76**, 110-114 (2015)

[13] H. Haftbaradaran, X. Xiao and H. Gao, Critical film thickness for fracture in thin-film electrodes on substrates in the presence of interfacial sliding. *Modelling Simul. Mater. Sci. Eng*, **21**, 074008, (2013)